Supporting Information

Aryl bis-sulfonamides bind to the active site of a homotrimeric isoprenoid biosynthesis enzyme IspF and extract the essential divalent metal cation cofactor

Katharina Root[a§], Konstantin Barylyuk[a§†], Anatol Schwab[a], Jonas Thelemann[a], Boris Illarionov[b], Julie Geist[a], Tobias Gräwert[b], Adelbert Bacher[c], Markus Fischer[b], François Diederich[a], Renato Zenobi[*a]

[a] Department of Chemistry and Applied Biosciences, ETH Zurich, Zurich, Switzerland
[b] Hamburg School of Food Science, University of Hamburg, Hamburg, Germany.
[c] Department of Chemistry, Technical University Munich (TUM), Garching, Germany.
§K.R. and K.B. contributed equally to this work.
† Present address: Department of Biochemistry, University of Cambridge, Hopkins building, Downing Site, Tennis Court Road, CB2, 1QW, United Kingdom.

Experimental

Materials

All chemicals used were of analytical grade or higher. Ammonium acetate (>99.0% for LC-MS), cesium iodide (Analytical standard for high-resolution mass spectrometry) and dimethylsulfoxide (DMSO) were purchased from Fluka Chemie AG (Buchs, Switzerland). Ultrapure water was obtained from Merck Millipore (Zug, Switzerland). Phenylmethanesulfonyl flouride (PMSF) and ethylenediaminetetraacetic acid (EDTA) were purchased from Sigma (Buchs, Switzerland). Recombinant IspF from *A. thaliana* was expressed and purified in-house.

Aryl bis-sulfonamide compounds (**8**, **9**, **10**, **11**, **12, 13**) were synthesized as in[1] and used without further purification. Stock solutions at a concentration of 50 mM were prepared in DMSO. The structures of the individual compounds, their molecular weight, IC_{50} values in complex with *At*IspF determined *in vitro*[1] are summarized in **Table SI1**.

Buffer Exchange. *At*IspF was buffer-exchanged against 200 mM ammonium acetate (pH = 8.0) overnight at 4°C at 600 rpm using Slide-A-Lyzer MINI dialysis devices MWCO 7000 Da (Thermo Scientific, Switzerland).

Determination of the Protein Concentration. The protein concentration was determined by measuring the absorbance at 280 nm with a Genesys 10S UV/Vis spectrophotometer (Thermo Scientific, Madison, WI, USA) using disposable plastic UV cuvettes (UVette, Vaudax-Eppendorf AG, Schönenbuch/Basel, Switzerland). Aqueous ammonium acetate solution (c = 200 mM; pH = 8.0) was used as a blank. The concentration of monomeric *At*IspF was calculated according to Beer-Lambert law (using the extinction coefficient ε_{280} = 8490 cm^{-1} M^{-1}).

Computational Docking Studies. The structure-based analysis was performed on the crystal structure of CMP-bound *At*IspF (PDB ID: 2PMP).[2] Representative for other substituents, **10** was chosen. Modeling of two ligands in the active site was performed using the program MOLOC,[3] and in line with the experimental results, binding without involvement of the catalytic zinc ion to the enzyme was assumed. Ligands were positioned to be in agreement with the previously reported structure-activity relationship,[1] and to account for the conformational preferences of their functional groups. The conformation of aryl-sulfonamides is strongly dictated by stereoelectronic and steric interactions, as evident from crystallographic data of the CSD database and DFT calculations (**Figure 5b**).[4, 5] The π-orbital of an aryl substituent on the sulfonamide favorably bisects the O=S=O angle, which has been accounted for by a C_{ar}–C_{ar}–S–N angle constraint of 90±15° in our modeling. Along the C–S–N–C dihedral a staggered conformation with the nitrogen lone pair bisecting the O=S=O angle is preferred, resulting in a *gauche* arrangement of carbon substituents on the nitrogen and sulfur atom. For this dihedral, the majority of CSD occurrences fall in a range of 60–90° which led us to assume 75±15° as a constraint. The sulfonamide groups are largely buried in the binding pocket and establish polar interactions with Lys135, Lys107 and Ser38, but also engage in hydrophobic contacts such as the C_{ar}–H···O interaction with the side chain phenyl of Phe79.

To account for the different spatial demand of the various inhibitors (**Scheme 2**), the substituted positions were oriented towards the periphery or allowed a suitable exit vector. Inhibitors bearing bromine substituents on the diamine scaffold constitute the most active derivatives of the ligand class. Superior inhibition and binding of bromide over the corresponding methyl derivatives, such as **10** vs. **13**, suggest favorable halogen bonding interactions of the two halide substituents.[6] In the modeled binding mode, one inhibitor establishes a halogen bond at a close to ideal geometry of 160° to

the backbone carbonyl group of Gly61. The second ligand positions the two bromine substituents at close distance above and below the side chain carboxylate of Glu138 such that a small rotation of the carboxylate in either direction would result in a similar, highly favorable interaction.[7, 8]

Table SI1: Key characteristics of the aryl bis-sulfonamide inhibitors of *At*IspF.[1]

Name	Molecular weight/ Da	IC_{50}/µM
8	732.10	0.24
9	704.05	0.53
10	574.31	5.6
11	555.79	53
12	485.97	133
13	444.57	>500

Metal Cation Extraction from *At*IspF

A stock protein solution at a concentration of 98 µM was mixed with EDTA (c = 1 mM, pH = 8.0) and stirred for 3 h at room temperature. The excess of EDTA was then removed by dialysis.

Protein Denaturation

In order to determine the exact mass of the protein using ESI-MS, 1µL of *At*IspF stock solution was diluted (1:10) in 1% (vol.) aqueous formic acid and loaded on ZipTip C18 (Millipore AG, Zug, Switzerland) preconditioned with acetonitrile and equilibrated with 1% aqueous formic acid. 30 µL of 1% aqueous formic acid was applied to wash the buffer salts and additives. This was followed by elution of the protein into 20µL of formic acid:acetonitrile:water 1:49.5:49.5 (vol.:vol.:vol.).

Mixing Scheme for the titration Experiments

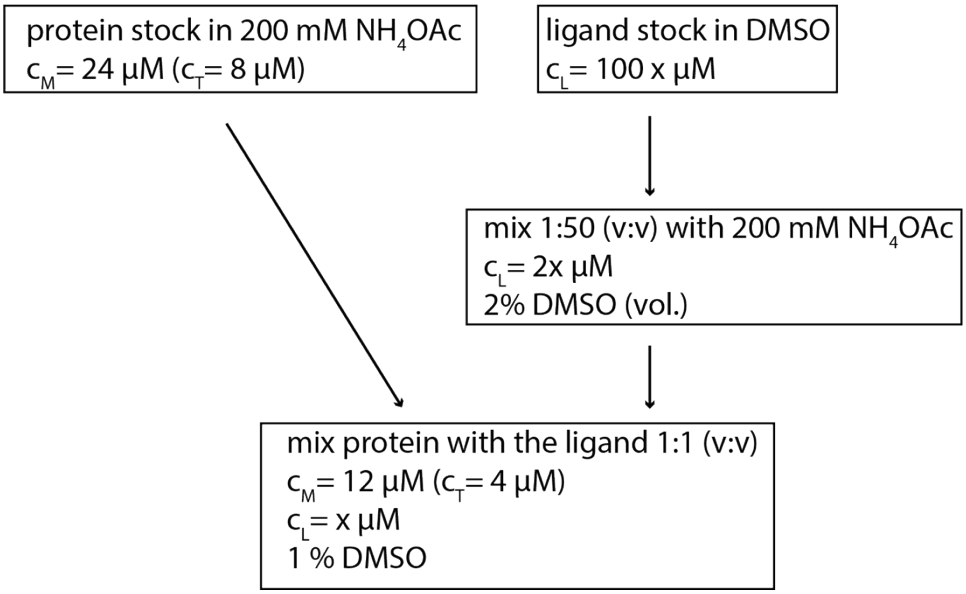

Scheme SI 1: Mixing scheme visualizing how the protein and ligand solutions were mixed for the titration experiments.

Data Analysis

All data analysis was done in MATLAB R2017a (MathWorks Inc., Natick, MA, USA). When necessary, the spectra were background-adjusted using *msbackadj* function from MATLAB Bioinformatics Toolbox and smoothed using Savitzky-Golay algorithm implemented in *sgolayfilt* MATLAB function. In Savitzky-Golay smoothing, the 2nd order polynomial function and a window of 9-25 samples were used. The spectra normalization was done using *msnorm* function from MATLAB Bioinformatics Toolbox.

Expression, Purification, and Characterization of Recombinant *At*IspF

Synthetic gene of the full-length wild-type (wt) IspF from *Arabidopsis thaliana* (*At*IspF; UniProt accession number ISPF_ARATH) fused at the N-terminus with the tobacco etch virus protease (TEV-protease) recognition site (ENLYF) was inserted into a Novagen pET-15b expression vector (Merck & Cie, Schaffhausen, Switzerland) at the NdeI and BamHI cloning sites. The gene synthesis and cloning into the expression vector was performed by GenScript (GenScript USA Inc., Piscataway, NJ, USA). The resulting recombinant product consisted of the N-terminal His_6-tag, a linker containing recognition sites for thrombin and TEV-protease, and wt *At*IspF

(**Scheme SI2**). The recombinant polypeptide was 205-amino-acid-residue-long and had a theoretical molecular weight of 22186.3 Da.

```
         10         20         30         40         50         60
MGSSHHHHHH SSGLVPRGSH MENLYFAASS AVDVNESVTS EKPTKTLPFR IGHGFDLHRL

         70         80         90        100        110        120
EPGYPLIIGG IVIPHDRGCE AHSDGDVLLH CVVDAILGAL GLPDIGQIFP DSDPKWKGAA

        130        140        150        160        170        180
SSVFIKEAVR LMDEAGYEIG NLDATLILQR PKISPHKETI RSNLSKLLGA DPSVVNLKAK

        190        200
THEKVDSLGE NRSIAAHTVI LLMKK
```

Scheme SI 2: Amino acid sequence of the recombinant fusion protein His_6-TEVrs-*At*IspF. The N-terminal His_6-tag sequence is highlighted in blue, the TEV-protease recognition site sequence is highlighted in red. The sequence of full-length mature wild-type IspF from *A. thaliana* (UniProt ID ISPF_ARATH; residues number 53-231 in UniProt notation) is shown in bold.

His_6-*At*IspF was expressed in soluble form in *E. coli* One Shot™ BL21 Star™ (DE3) host cells (Life Technologies Europe B.V., Zug, Switzerland). Cells were precultured in 10 ml of LB broth containing 0.1 g L^{-1} ampicillin for 12 h at 37 °C with agitation (240 rpm, orbital shaker). The starting culture was inoculated into 2 L of LB broth containing 0.1 g L^{-1} ampicillin and was cultured at 37 °C with continuous agitation (120 rpm, orbital shaker) for approximately 3.5 h until reached $OD_{600\ nm}$ = 0.8. The expression of the target transgene was induced by adding IPTG to a final concentration of 1 mM. The expression was performed for 4 h at 37 °C with continuous agitation (120 rpm, orbital shaker). The cells were harvested by centrifugation and stored at -80 °C until used.

For extraction of the recombinant fusion protein, the cells were resuspended in a lysis buffer (50 mM Tris-HCl, pH 8.0, 100 mM NaCl, 20 mM imidazole, 1 mg mL^{-1} lysozyme, 0.1 mM PMSF, 1 mM DTT) at a proportion of 10 ml buffer per 1 g of wet cell paste and lysed by two consecutive passages through a high-pressure fluid processor Microfluidizer 110S (Microfluidics, Newton, Massachusetts, USA) operated at 40 psi. The homogenate was centrifuged at 25,000 rpm (rotor 45 Ti, Optima L-90 K Ultracentrifuge, Beckman Coulter, Inc.), +4 °C for 1 h. The supernatant containing soluble proteins was collected and processed further.

143 The target product was isolated from the soluble fraction of host cell lysate by Ni-
144 chelate chromatography on a GE HisTrap-FF column (5 ml bed volume; GE
145 Healthcare, Glattbrugg, Switzerland) using an Akta Prime Plus FPLC system (GE
146 Healthcare, Glattbrugg, Switzerland) equipped with dual-channel fluidics and a UV
147 absorbance and conductivity detectors. The column was equilibrated in elution buffer
148 A (50 mM Tris-HCl, pH 8.0, 100 mM NaCl, 20 mM imidazole, 0.5 mM DTT) at a
149 flow rate of 5 mL min^{-1}. After the protein extract was loaded on the column and the
150 $A_{280\ nm}$ reading returned to the base line, the protein captured on the Ni-NTA resin
151 was eluted with elution buffer B (50 mM Tris-HCl, pH 8.0, 100 mM NaCl, 300 mM
152 imidazole, 0.5 mM DTT) (**Scheme SI3a**). The concentration of imidazole in the
153 eluate was reduced back to 20 mM by desalting on a GE HighPrep 26/10 size-
154 exclusion column (MWCO = 5 kDa; GE Healthcare, Glattbrugg, Switzerland)
155 equilibrated in elution buffer A **Scheme SI3b**).
156 The His_6-TEVrs-*At*IspF fusion protein was digested with the recombinant catalytic
157 domain of TEV-protease to cleave the N-terminal His_6-tag. After 4 h incubation at
158 room temperature, the reaction mixture was subjected to another round of Ni-chelate
159 chromatography in order to remove the uncleaved fusion protein, the His_6-tag-
160 containing N-terminal fragment, and the TEV-protease, which also carried N-terminal
161 His_6-tag (**Scheme SI3c**). The flow-through fraction from the GE HisTrap-FF column
162 contained high-purity full-length wt *At*IspF (**Scheme SI3d**). Overall, the cloning,
163 expression, and purification strategy used here yielded approximately 18 mg of *At*IspF
164 per 1 L of bacterial culture. The coupled-enzyme photometric assay confirmed that
165 the purified enzyme was active. The turnover numbers measured for two *At*IspF
166 samples purified in separate batches were 5.9 min^{-1} and 6.8 min^{-1}. The purified
167 enzyme was also sensitive to synthetic *bis*-sulfonamide inhibitors in the standard IC_{50}
168 assay.[9]
169

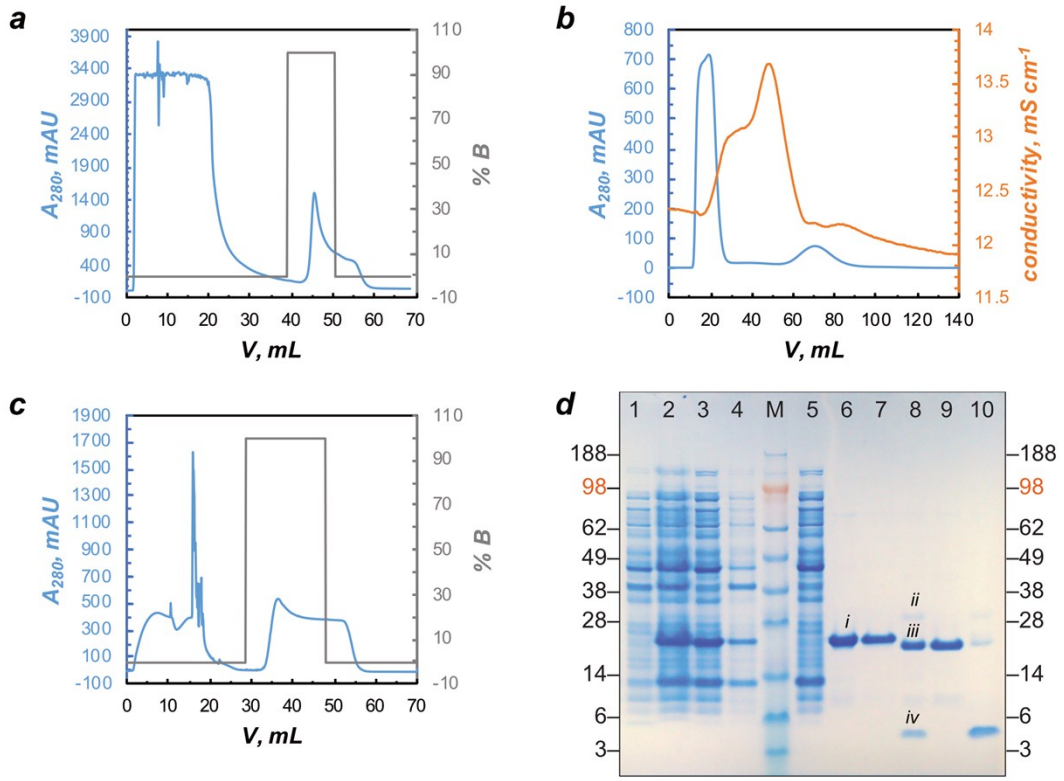

Scheme SI 3: Expression and purification of the recombinant *At*IspF. (*a*) Elution profile from the first Ni-chelate chromatography step. (*b*) SEC elution profile of the eluate fraction obtained from the first Ni-chelate chromatography. (*c*) Elution profile of the TEV-protease digest from the second Ni-chelate chromatography step. (*d*) Analysis of protein fractions sampled from consecutive steps of the protein expression and purification workflow by SDS-PAGE (4-12 % Bis-Tris NuPAGE Mini Gel, NuPAGE MES SDS running buffer; Life Technologies Europe B.V., Zug, Switzerland). 1: whole-cell lysate before induction of the transgene expression; 2: whole-cell lysate 4 h post induction; 3: soluble protein fraction; 4: insoluble protein fraction; 5: flow-through fraction from the first Ni-chelate chromatography step; 6: eluate from the first Ni-chelate chromatography step highly enriched in the target fusion protein (band *i*); 7: void-volume fraction collected from the SEC column; 8: TEV-protease digest containing a minor amount of TEV-protease (band *ii*) and the two products of digestion, the full-length *At*IspF and the N-terminal His_6-tag-containing peptide (bands *iii* and *iv*, respectively); 9: flow-through fraction collected from the second Ni-chelate chromatography step containing highly pure tag-less *At*IspF; 10: eluate from the second Ni-chelate chromatography step; M – molecular weight standards (SeeBlue Plus 2, Life Technologies Europe B.V., Zug, Switzerland). The molecular weights of the MW standards are indicated on the sides in kDa.

Molecular Weight of *At*IspF Measured by ESI-MS

The spectrum of denatured protein showed a typical broad distribution of peaks in a relatively low *m/z* range (**Figure SI1**). The measured mass (19225.0 ± 0.3 Da) corresponds to the theoretical molecular weight (19225.1 Da) calculated based on the amino acid sequence (**Table SI2**). As expected, no non-covalent protein complexes survived under denaturing conditions and all the spectral signals were matched to unfolded monomeric protein ions.

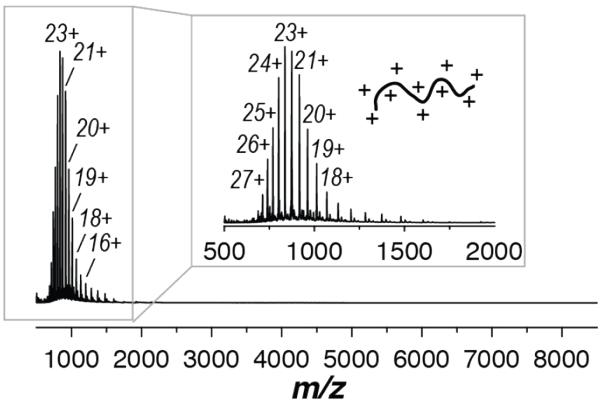

Figure SI 1: ESI mass spectrum acquired under denaturing conditions in positive ion mode. The broad charge state distribution shows the unfolded *At*IspF monomer in the low *m/z* range.

Table SI2: – Molecular weight of bare *At*IspF using denaturing- and native ESI-MS.

		Monomer	Dimer	Trimer
	Theoretical	19225.1	38450.2	57675.3
ESI	Denaturing	19225.0 ± 0.3	-	-
	Native	19224.1 ± 1.0	38449.2 ± 7.1	57680.7 ± 5.4
	CID	19224.03 ± 0.4	38451.20 ± 2.1	-

Experimentally estimated masses of neutral species were calculated from *m/z* values of multiply-charged ions attributed to monomers, dimers, and trimers in **Figure 1**. These values are compared to theoretical molecular weights calculated from amino acid sequences. Deviations between experimental and theoretical values are indicated.

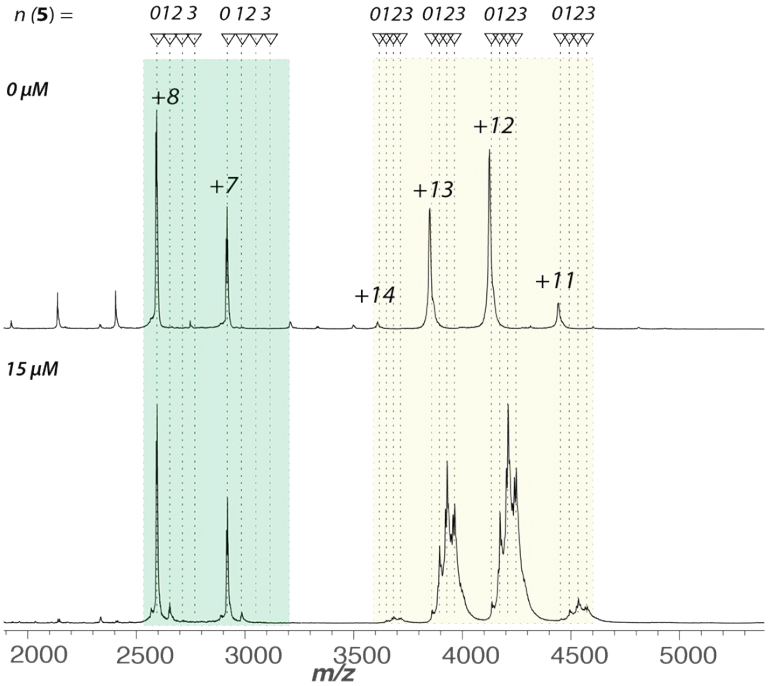

Figure SI 2: Evaluation of non-specific binding of CDP-ME to *At*IspF. PMSF-inactivated trypsin was mixed with *At*IspF and measured before incubation (top spectrum) and after incubation (bottom spectrum) with CDP-ME. Associated signals are highlighted in yellow boxes and were attributed to trypsin (left box, green) and *At*IspF (right box, yellow). Upon CDP-ME addition, mass shifts corresponding to 1, 2 or 3 CDP-ME molecules bound to *At*IspF trimer (indicated by dotted lines) were observed exclusively. Negligible complex formation by CDP-ME and trypsin was detected.

Formation of nonspecific ligated states is well known in ESI-MS and originates from ligands sticking to the protein surface upon droplet shrinkage.[10] ESI-born non-specific ligand binding due to electrostatic attraction has been shown to proceed equally for all protein ions, regardless of their molecular weight.[10] Therefore, to rule out the possibility of nonspecific binding of the substrate to *At*IspF, we added PMSF-inactivated trypsin as a reference protein (P^{REF}) to the mixture of *At*IspF with **7** (**Figure SI2**). We expected to detect complexes of trypsin with **5** or **7** should ESI-related nonspecific binding be pronounced.

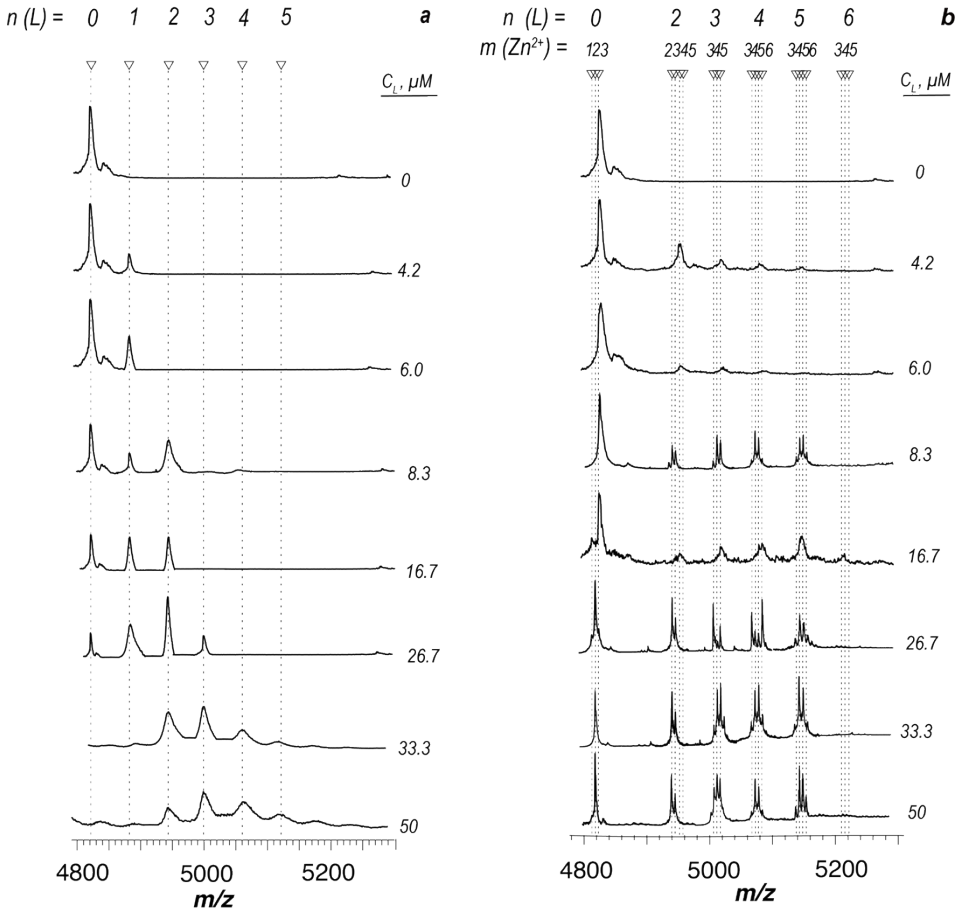

Figure SI 3: Titration series of *At*IspF (c_{trimer} = 8 µM) mixed with compound 8 (*L*) in the absence (a) and presence (b) of Zn^{2+}(150 mM ammonium acetate, 1% DMSO, pH = 8.0, positive mode). a) *At*IspF was incubated with 8 in the absence of Zn^{2+} resulting in complexes containing up to 6 ligands. The signal distribution shows subsequent binding of the ligands, which suggests that all 6 binding sites are equivalent. b) Zn^{2+} saturated *At*IspF (3:1) was mixed with increasing concentrations of 8 (T:L ratio increasing from 1:0 to 1:7). The Zn^{2+}: protein ratio gets scrambled upon increasing the *L* concentration. Zn^{2+} depleted states are observed for the ligand-free protein peak, 1:1 and 1:2 protein-ligand complex peaks (containing 2, 1, 0 Zn^{2+} ions). Further, for ligand-bound states 1:3 onwards a superstoichiometric number of Zn^{2+} ions bound was observed.

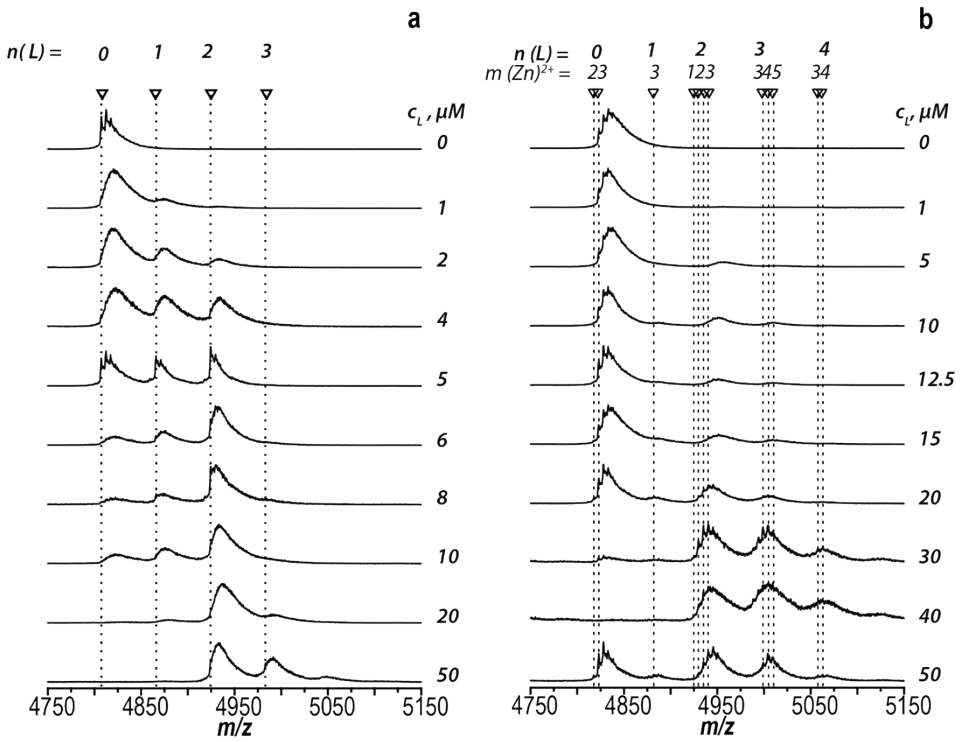

Figure SI 4: Titration series of *At*IspF (c_{trimer} = 8 µM) mixed with 9 in the absence (a) and presence (b) of Zn^{2+} (150 mM ammonium acetate, 1% DMSO, pH = 8.0, positive mode). a) *At*IspF was incubated with 9 in the absence of Zn^{2+} resulting in complexes containing up to 6 ligands. The signal distribution shows subsequent binding of the ligands, which suggests that all 6 binding sites are equivalent. b) Zn^{2+} saturated *At*IspF (3:1) was mixed with increasing concentrations of 9 (c_L = 0-50 µM). The Zn^{2+}: protein ratio gets scrambled upon increasing the bis-sulfonamide concentration. Zn^{2+} depleted states are observed for the ligand-free protein peak, 1:1 and 1:2 protein-ligand complex peaks (containing 2,1,0 Zn^{2+} ions). Further, for ligand-bound states 1:3 onwards a superstoichiometric number of 4-6 Zn^{2+} ions bound were observed.

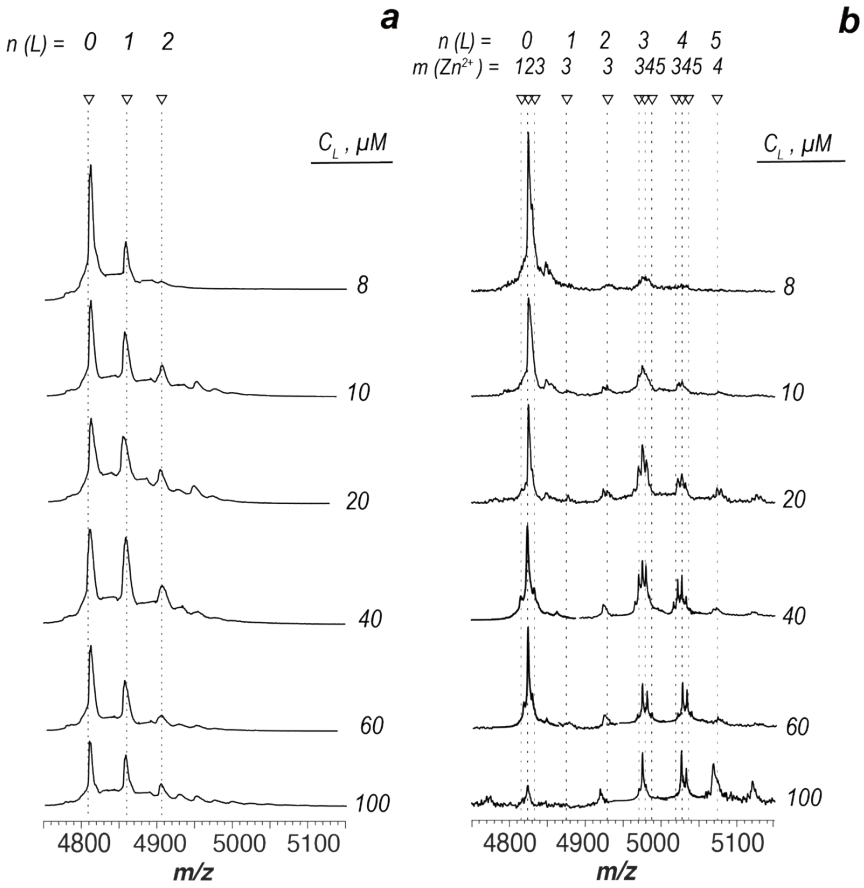

Figure SI 5: Titration series of *At*IspF (c_{trimer} = 8 µM) mixed with 11 in the absence (a) and presence (b) of Zn^{2+}(150 mM ammonium acetate, 1% DMSO, pH = 8.0, positive mode). a) *At*IspF was incubated with 11 in the absence of Zn^{2+} resulting in complexes containing up to 6 ligands. The signal distribution shows subsequent binding of the ligands, which suggests that all 6 binding sites are equivalent. b) Zn^{2+} saturated *At*IspF (3:1) was mixed with increasing concentrations of 11 (c_L = 0-100 µM). The Zn^{2+}: protein ratio gets scrambled upon increasing the bis-sulfonamide concentration. Zn^{2+} depleted states are observed for the ligand-free protein peak, 1:1 and 1:2 protein-ligand complex peaks (containing 2,1,0 Zn^{2+} ions). Further, for ligand-bound states 1:3 onwards a superstoichiometric number of 4-6 Zn^{2+} ions bound were observed.

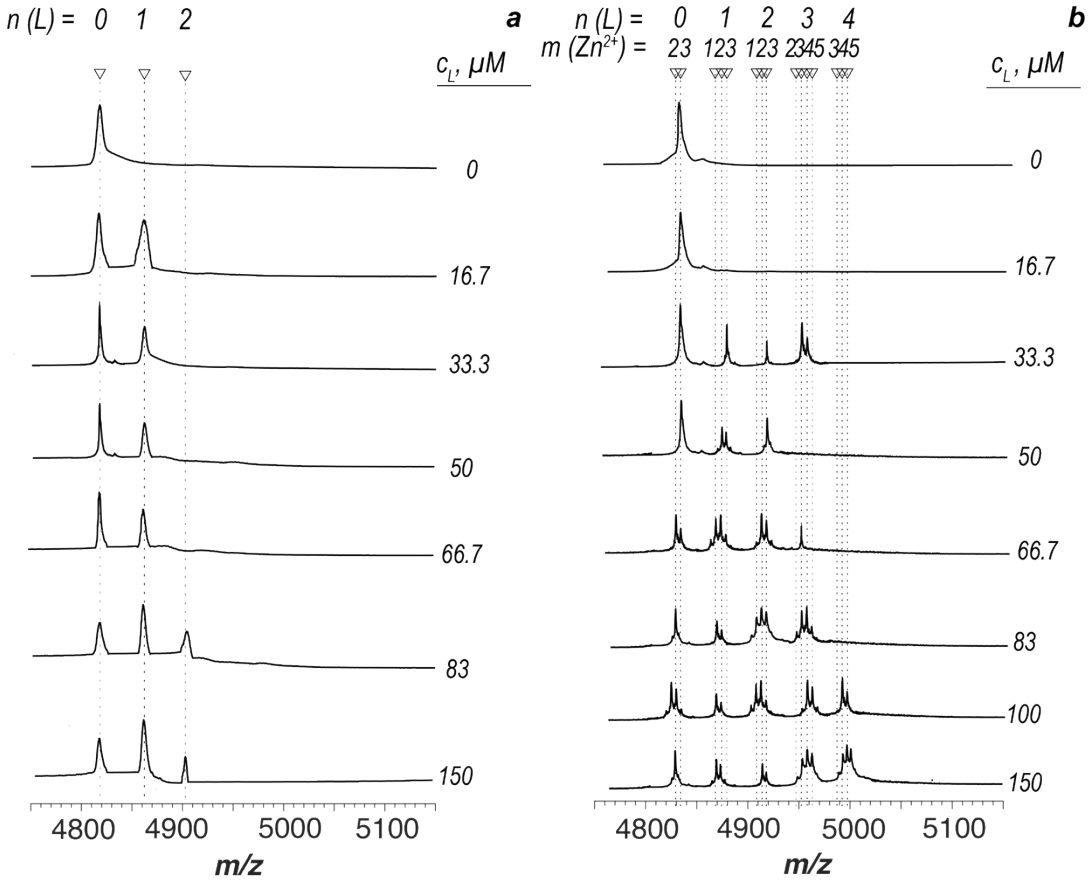

Figure SI 6: Titration series of *At*IspF (c_{trimer} = 8 μM) mixed with 12 in the absence (a) and presence (b) of Zn^{2+}. a) *At*IspF was incubated with 12 in the absence of Zn^{2+} resulting in complexes containing up to 6 ligands. The signal distribution shows subsequent binding of the ligands, which suggests that all 6 binding sites are equivalent. b) Zn^{2+} saturated *At*IspF (3:1) was mixed with increasing concentrations of 12 (c_L = 0-100 μM). The Zn^{2+}: protein ratio gets scrambled upon increasing the sulfonamide concentration. Zn^{2+} depleted states are observed for the ligand-free protein peak, 1:1 and 1:2 protein-ligand complex peaks (containing 2,1,0 Zn^{2+} ions). Further, for ligand-bound states 1:3 onwards a superstoichiometric number of 4-6 Zn^{2+} ions bound were observed.

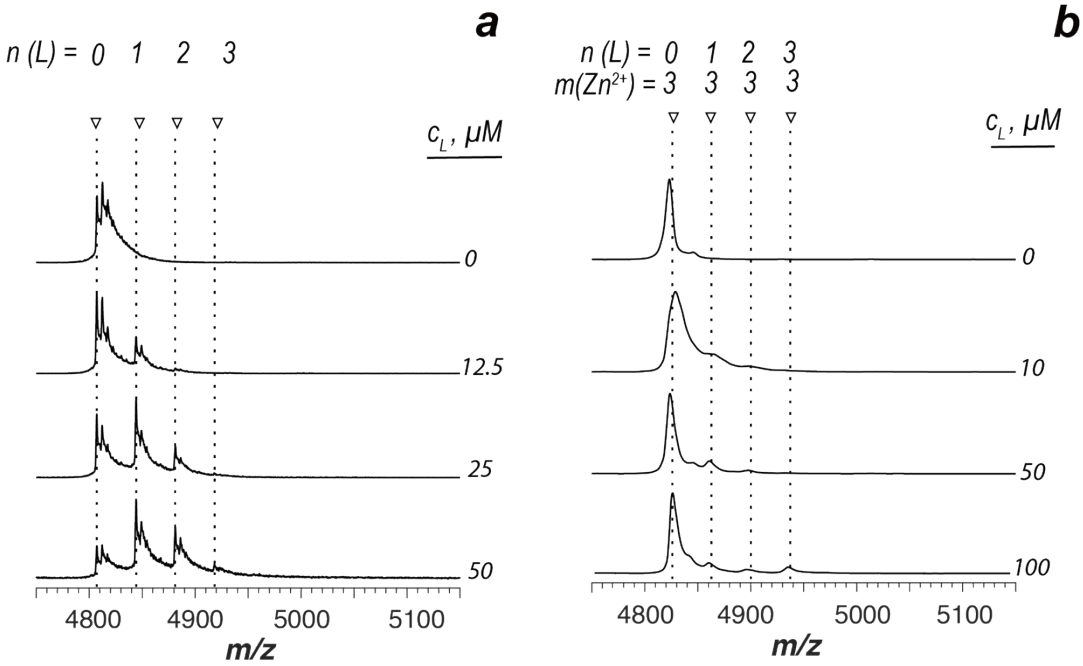

Figure SI 7: Titration series of *At*IspF (c_{trimer} = 8 µM) mixed with increasing concentrations of compound 13 in the absence (a) and presence (b) of Zn^{2+} (150 mM ammonium acetate, 1% DMSO, pH = 8.0, positive mode) that was used as a negative control, since it previously showed no inhibition in kinetic assays. a) *At*IspF was incubated with 13 in the absence of Zn^{2+} resulting in complexes containing up to 6 ligands. The signal distribution shows subsequent binding of the ligands. b) In the presence of Zn^{2+}, nearly no complex formation was observed. A less intense complex formation was observed in the presence of Zn^{2+} compared to when no Zn^{2+} was added. This suggests that Zn^{2+} ion alters the binding properties of the ligand.

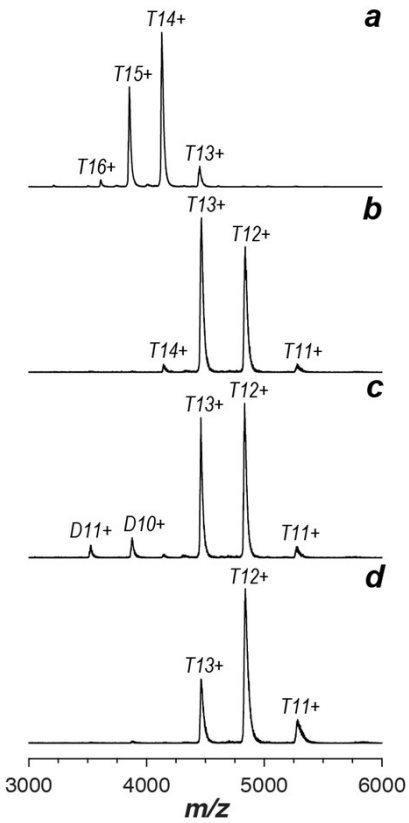

Figure SI 8: Titration of *At*IspF with increasing concentrations of DMSO (0-1% v/v). A mass spectrum of *At*IspF without DMSO is given for reference (a). Increasing the DMSO concentration up to 1 % results in a shift of the charge state distribution to lower charge states as well as peak broadening.

The charge state distribution (CSD) of native-like protein ions shifts to a lower number of charges upon the addition of DMSO.[11] Accordingly, we observed a shift of CSD of *At*IspF from the dominant trimer signal carrying *14+* charges in the absence of DMSO to *12+* charges in the presence of 1% DMSO (**Figure SI8**).

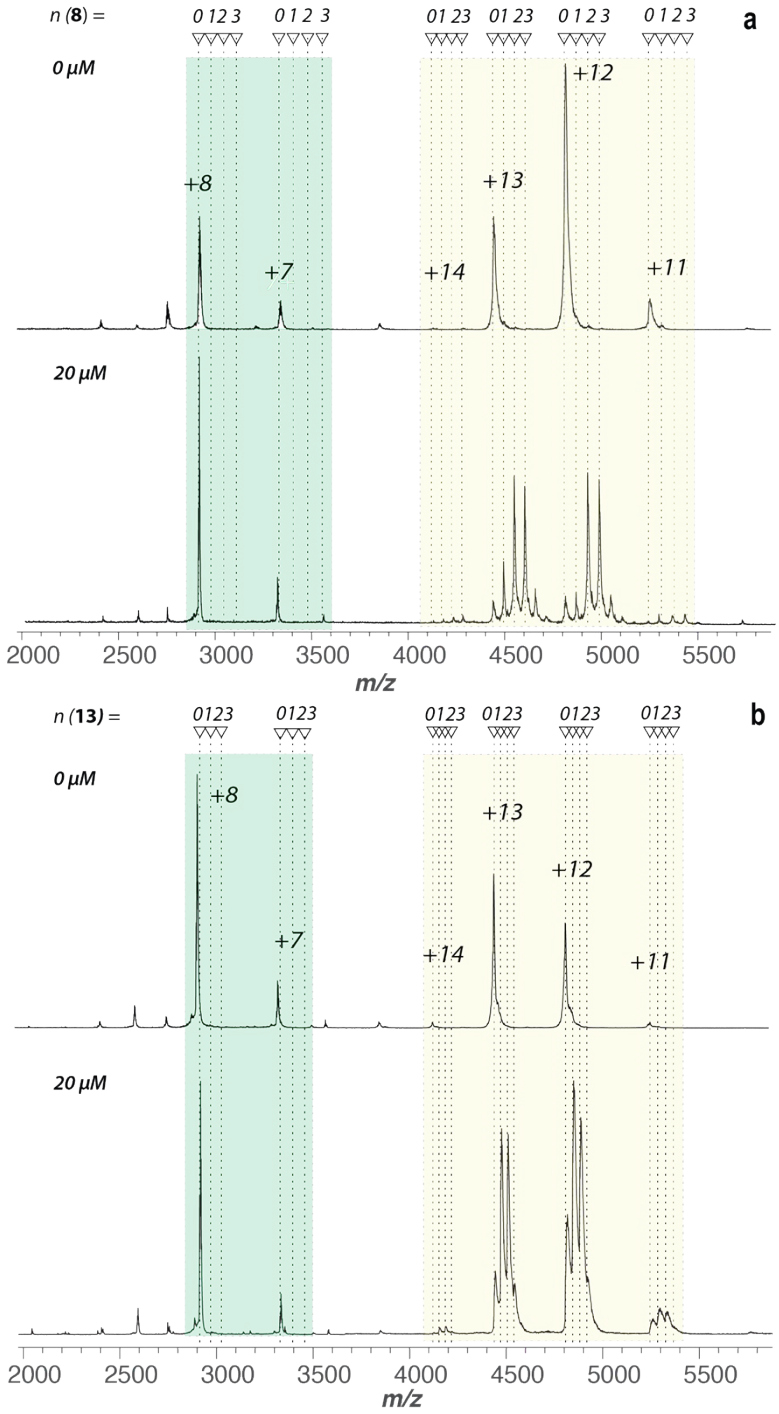

Figure SI 9: Evaluation of non-specific binding of 8 and inactive 13 to *At*IspF. PMSF-inactivated trypsin was mixed with *At*IspF alone (top spectra in a and b) and upon incubation (bottom spectra in a and b) with 8 and 13, respectively. Associated were attributed to trypsin (left box, green) and *At*IspF (right box, yellow). Upon the addition of 8, mass shifts corresponding to up to three molecules 8 bound to *At*IspF trimer exclusively (indicated by dotted lines) were observed. Contrarily, no complex formation by 8 or 13 and trypsin was detected, respectively.

To determine the fraction of nonspecific protein-ligand complexes (**8** and **13**, respectively) generated during the electrospray process, PMSF-inactivated trypsin was added to the mixture as a reference protein (P^{REF}) (**Figure SI9**). However, no ligated states were observed for P^{REF} with either compound. Thus, we can conclude

that the complexes between bis-sulfonamides and *At*IspF (in the absence of Zn^{2+}) are not due to ESI artifacts but are indeed present in solution.

ESI-MS Detects [8–Zn]$^{2-}$ Chelate Complex in Solution

X-Ray crystallography demonstrated that the bis-sulfonamide inhibitors form a dimeric chelation complex with Zn^{2+} ion [1]. **Figure SI10** shows the mass spectrum of **8** incubated with Zn^{2+} at a 2:1 ratio in positive ion mode. After mixing the ligand with Zn^{2+} a signal distribution next to the bare ligand corresponding to the chelated Zn^{2+} complex dominates the spectrum. The signal distributions corresponding to the bare ligand as well as the chelated complex are zoomed in and compared with theoretical signal distributions, which are shown below the spectrum for comparison. The results suggest, that ligand **8** exists in solution in a free and Zn^{2+} -bound forms. Bis-sulfonamides are known to chelate Zn^{2+} ions with association constants (K_a) of 15.6×10^6 M^{-2}.[1]

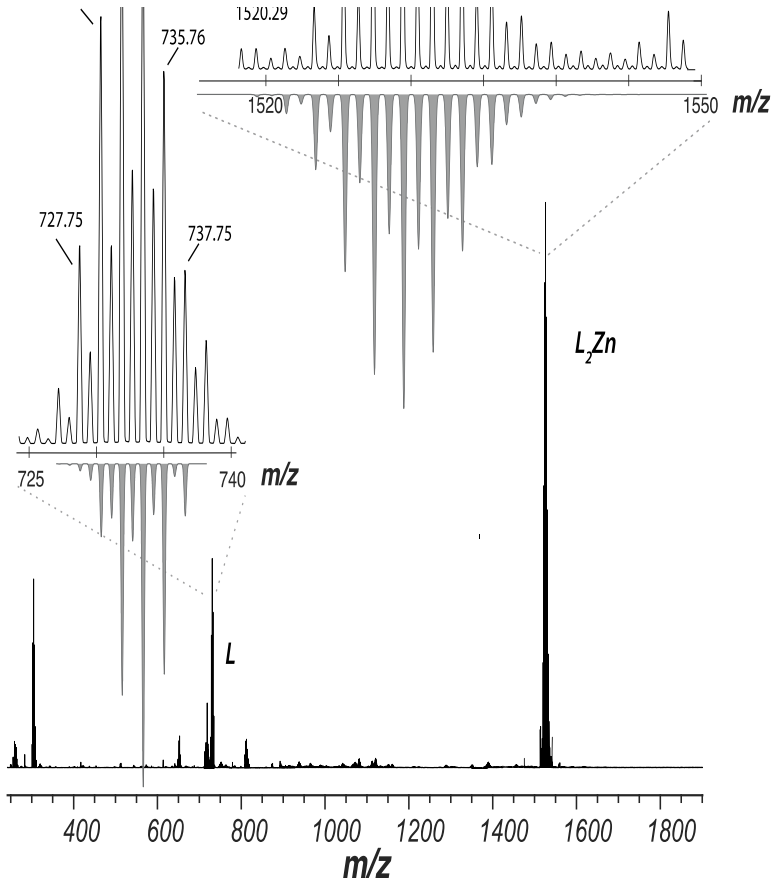

Figure SI 10: Comparison of a simulated and measured native ESI mass spectra of 8 mixed with Zn^{2+} at a 2:1 ratio (150 mM ammonium acetate, pH=8.0, positive mode). The simulated isotopic distribution is shown in grey. Insets show zoomed in signal distributions of the bare 8, as well as the chelated 2:1 complex with Zn^{2+}.

Docking of Bis-Sulfonamide Ligands in the Presence of Zn

Bis-sulfonamide ligands have previously been shown to form a dianionic 2:1 complex with Zn^{2+} upon deprotonation of the sulfonamide N-H.[1] While Zn^{2+} cofactor depletion might be a possible mode of inhibition, enzymatic assays in the presence of excess Zn^{2+} have shown undiminished inhibition and suggest complex binding to the active site. The crystal structure of the $[L_2Zn]^{2-}$ complex with ligand **10** shows a tetrahedral coordination with the Zn^{2+} ion. This complex was successfully modeled in the active site of *At*IspF (PDB ID: 2PMP, **Figure S11a**). For the model the coordination geometry of the Zn^{2+} was constrained. For the Zn^{2+}, as well as for the Zn-free binding mode, conformational preferences of the aryl-sulfonamide were taken into account (**Figure S11b**).

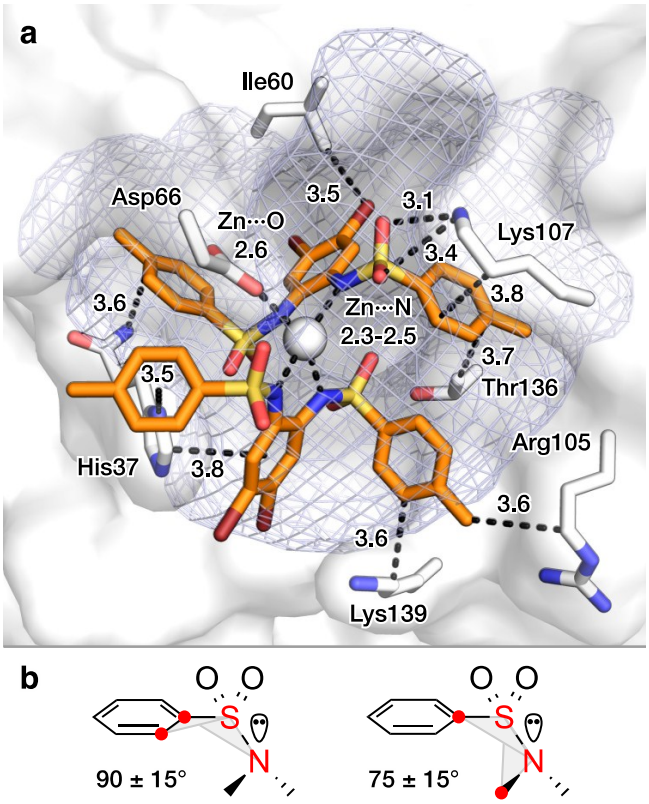

Figure SI11: Proposed binding mode of the $[L_2Zn]^{2-}$ complex with 10 in the active site of *At*IspF (a, PDB ID: 2PMP,[2] 2.3 Å), including conformational constraints for aryl sulfonamides (b). The mesh surface spans the volume of the active site.[12] Atom coloring: Br brown, N blue, O red, S yellow, distances are given in Å.

The binding mode of the $[L_2Zn]^{2-}$ complex of **10** shows coordination of the zinc ion with Asp66, which is similar to the binding mode of CDP, where a

342 magnesium ion binds to the diphosphate moiety and to Asp66.[13] One ligand
343 molecule of **10** is deeply buried in the pocket, while the other partially
344 protrudes into the bulk. The buried ligand shows aromatic stacking interactions
345 of one tolyl substituent to the backbone amide of His37, while the other tolyl is
346 sandwiched between side-chains of Thr136 and Lys107. The latter possibly
347 also displays cation-π interactions with Lys107. The more exposed ligand has
348 two edge-to-face interactions of the tolyl and dibromobenzyl moieties with the
349 His37 side chain. The second tolyl group of this ligand has Van-der-Waals
350 interactions with the side chains of Thr136, Arg105 and Lys139.
351
352
353 **References**

354 1. Thelemann J, Illarionov B, Barylyuk K, Geist J, Kirchmair J, Schneider P, et
355 al. Aryl Bis-Sulfonamide Inhibitors of IspF from Arabidopsis thaliana and
356 Plasmodium falciparum. ChemMedChem. 2015;10(12):2090-8. doi:
357 10.1002/cmdc.201500382. PubMed PMID: 26435072.
358 2. Calisto BM, Perez-Gil J, Bergua M, Querol-Audi J, Fita I, Imperial S.
359 Biosynthesis of isoprenoids in plants: structure of the 2C-methyl-D-erithrytol
360 2,4-cyclodiphosphate synthase from Arabidopsis thaliana. Comparison with the
361 bacterial enzymes. Protein Sci. 2007;16(9):2082-8. doi: 10.1110/ps.072972807.
362 PubMed PMID: 17660251; PubMed Central PMCID: PMCPMC2206962.
363 3. Gerber PR, Muller K. Mab, a Generally Applicable Molecular-Force Field
364 for Structure Modeling in Medicinal Chemistry. J Comput Aided Mol Des.
365 1995;9(3):251-68. doi: Doi 10.1007/Bf00124456. PubMed PMID:
366 WOS:A1995RG92700005.
367 4. Schwertz G, Frei MS, Witschel MC, Rottmann M, Leartsakulpanich U,
368 Chitnumsub P, et al. Conformational Aspects in the Design of Inhibitors for Serine
369 Hydroxymethyltransferase (SHMT): Biphenyl, Aryl Sulfonamide, and Aryl
370 Sulfone Motifs. Chem-Eur J. 2017;23(57):14345-57. doi:
371 10.1002/chem.201703244. PubMed PMID: WOS:000412819400032.
372 5. Brameld KA, Kuhn B, Reuter DC, Stahl M. Small molecule conformational
373 preferences derived from crystal structure data. A medicinal chemistry focused
374 analysis. J Chem Inf Model. 2008;48(1):1-24. doi: 10.1021/ci7002494. PubMed
375 PMID: WOS:000252713700001.
376 6. Cavallo G, Metrangolo P, Milani R, Pilati T, Priimagi A, Resnati G, et al. The
377 Halogen Bond. Chem Rev. 2016;116(4):2478-601. doi:
378 10.1021/acs.chemrev.5b00484. PubMed PMID: WOS:000371106000018.
379 7. Zimmermann MO, Lange A, Zahn S, Exner TE, Boeckler FM. Using Surface
380 Scans for the Evaluation of Halogen Bonds toward the Side Chains of Aspartate,
381 Asparagine, Glutamate, and Glutamine. J Chem Inf Model. 2016;56(7):1373-83.
382 doi: 10.1021/acs.jcim.6b00075. PubMed PMID: WOS:000380422500013.
383 8. Schwab A, Illarionov B, Frank A, Kunfermann A, Seet M, Bacher A, et al.
384 Mechanism of Allosteric Inhibition of the Enzyme IspD by Three Different Classes

385 of Ligands. ACS Chem Biol. 2017;12(8):2132-8. doi:
386 10.1021/acschembio.7b00004. PubMed PMID: 28686408.
387 9. Illarionova V, Kaiser J, Ostrozhenkova E, Bacher A, Fischer M, Eisenreich
388 W, et al. Nonmevalonate terpene biosynthesis enzymes as antiinfective drug
389 targets: substrate synthesis and high-throughput screening methods. J Org Chem.
390 2006;71(23):8824-34. doi: 10.1021/jo061466o. PubMed PMID: 17081012.
391 10. Sun N, Sun J, Kitova EN, Klassen JS. Identifying nonspecific ligand binding
392 in electrospray ionization mass spectrometry using the reporter molecule
393 method. J Am Soc Mass Spectrom. 2009;20(7):1242-50. doi:
394 10.1016/j.jasms.2009.02.024. PubMed PMID: 19321359.
395 11. Sterling HJ, Prell JS, Cassou CA, Williams ER. Protein conformation and
396 supercharging with DMSO from aqueous solution. J Am Soc Mass Spectrom.
397 2011;22(7):1178-86. doi: 10.1007/s13361-011-0116-x. PubMed PMID:
398 21953100; PubMed Central PMCID: PMCPMC3107942.
399 12. Ho BK, Gruswitz F. HOLLOW: generating accurate representations of
400 channel and interior surfaces in molecular structures. BMC Struct Biol.
401 2008;8:49. doi: 10.1186/1472-6807-8-49. PubMed PMID: 19014592; PubMed
402 Central PMCID: PMCPMC2603037.
403 13. Kemp LE, Bond CS, Hunter WN. Structure of 2C-methyl-D-erythritol 2,4-
404 cyclodiphosphate synthase: an essential enzyme for isoprenoid biosynthesis and
405 target for antimicrobial drug development. Proc Natl Acad Sci U S A.
406 2002;99(10):6591-6. doi: 10.1073/pnas.102679799. PubMed PMID: 11997478;
407 PubMed Central PMCID: PMCPMC124447.
408